



## On the formation of small-scale irregularities driven by auroral particle precipitation

Florine Enengl<sup>(1)</sup>, Luca Spogli<sup>(2,5)</sup>, Daria Kotova<sup>(1)</sup>, Yaqi Jin<sup>(1)</sup>, Kjellmar Oksavik<sup>(3,4)</sup>, Noora Partamies<sup>(3,4)</sup>, Wojciech J. Miloch<sup>(1)</sup>

(1) Department of Physics, University of Oslo, PO Box 1048, Blindern, 0316 Oslo, Norway

(2) Istituto Nazionale di Geofisica e Vulcanologia, Via di Vigna Murata 605, 00143 Rome, Italy

(3) Birkeland Centre for Space Science, Department of Physics and Technology, University of Bergen, PO Box 7803, 5020 Bergen, Norway

(4) University Centre in Svalbard, N-9171 Longyearbyen, Norway

(5) SpacEarth Technology, Via di Vigna Murata 605, 00143 Rome, Italy

### Abstract

Ionospheric plasma structuring processes and irregularities can be caused by precipitating particles. Radio waves propagating through electron density irregularities may undergo rapid fluctuations of phase and amplitude. Phase fluctuations can be caused by refraction, due to ionospheric irregularities covering the full range of scale size: from cm's up to hundreds of km's. A peculiar kind of fluctuations are those due to the diffraction of the signal through irregularities below the Fresnel's scale and are called "scintillation", which affect both amplitude and phase of the received wave. Scintillation and phase fluctuations are commonly monitored through the amplitude and phase scintillation indices. In this paper we aim to understand the contribution of diffractive variations involved in particle precipitation events and resulting in scintillation events recorded by ground-based Global Navigation Satellite Systems (GNSS) receivers. We study multiple cases of different auroral forms and auroral intensity and how they lead to the formation of small-scale irregularities.

### 1 Introduction

Radio waves propagating through the ionosphere may encounter electron density irregularities along the signal path, which can lead to rapid fluctuations in phase and amplitude [1]. The size of the irregularities can determine the refractive and/or diffractive contribution in the recorded fluctuations of the amplitude and phase of radio wave signals. When a radio wave propagates through plasma structure below the Fresnel scale diffraction occurs that impacts the signal amplitude and phase. Refraction may occur due to density irregularities of any scale size and affect the signal phase [1,2]. When filtering GNSS data, it is commonly attempted to remove the refractive effects. A proper treatment of the GNSS is needed to efficiently disentangle the refractive and diffractive contributions [3,4]. In this study the focus is on the diffractive contributions to the received signals, quantified by the amplitude scintillation index (S4) and the ionospheric free linear combination (IFLC), which accounts for the 1<sup>st</sup> order

refractive contribution. We aim to describe the conditions leading to small-scale irregularities and variations in S4 and IFLC. For this, we study multiple cases of different auroral forms and intensities in relation to the indices to understand a possible role of particle precipitation in small-scale irregularity formation. We will further use additional data sources of electron density and flux measurements to describe the plasma irregularity conditions.

### 2 Instrumentation

To characterize the particle precipitation events, we utilize all-sky imagers. To quantify refractive and diffractive variations we use scintillation receiver raw data, power and phase, and compute the phase and amplitude scintillation index. The All-Sky Imager is a Keo Sentry 4ix Monochromatic Imagers from KEO Scientific with filters operated by the University of Oslo (UiO) in Longyearbyen (LYR, geographic coordinates: 78.15°N, 16.04°E). The scintillation receiver PolaRxS/PolaRx5s [5] is operated by the Istituto Nazionale di Geofisica and Vulcanologia (INGV) and situated in Longyearbyen (LYR, geographic coordinates: 78.17° N, 15.99° E.) [6].

### 2 Analysis

The scintillation receiver in Longyearbyen (LYR) has been operational since the 2019 season, data onwards have been considered in this study. All-sky imager (ASI) data from the season 2019/2020 of different auroral forms are analyzed and compared. An auroral event as observed with the ASI classified as 'Large Vortex' and the green emissions (557.7nm) are shown together with the positions of GNSS satellites in Fig.1. Corresponding scintillation receiver recordings of S4, the phase scintillation index  $\sigma_\phi$  and the IFLC of this event are shown in Fig.2. The S4 index is given as the ratio of the standard deviation of the signal intensity (I) to the average intensity:

$$S_4 = \sqrt{\frac{\langle I^2 \rangle - \langle I \rangle^2}{\langle I \rangle^2}} \quad (1)$$

The  $\sigma_\phi$  index is the standard deviation of the detrended measured phase:

$$\sigma_\phi = \langle \phi^2 \rangle - \langle \phi \rangle^2. \quad (2)$$

The cut-off frequency applied for phase detrending is the standard 0.1 Hz, which is not effective in minimizing the contribution of the refraction contribution in the  $\sigma_\phi$  calculation [4]. The simultaneous use of the standard  $\sigma_\phi$  and S4 can support the speculation about the scale-size of the irregularities involved.

Additionally, the ionospheric free linear combination is calculated using the carrier frequencies of two signals given by:

$$IFLC = \frac{f_1^2 \phi_{L1} - f_2^2 \phi_{L2}}{f_1^2 - f_2^2}. \quad (3)$$

In (3),  $\phi_1$  and  $\phi_2$  are the phases of two ( $f_1, f_2$ ) GNSS central frequencies, respectively. The scintillation receiver data is used in a resolution of 50 Hz and integrated over 1 second to compute the indices.

### 3 Results and Discussion

A selected event classified as ‘Large Vortex’ from 22<sup>nd</sup> February 2020 is presented in Fig. 1. It shows the green auroral emissions as recorded by the ASI data. The positions of the GNSS satellites are projected onto the ASI image. Galileo satellite SVID #83 is situated in the center of Fig. 1. as indicated by the red circle and is seen within the auroral emissions at the time of the plot (19:20 UT). The recorded data by the scintillation receiver in LYR for satellite #83 is shown in Fig.2. The S4 index, see panel a), is elevated from 19:18 UT – 19:28 UT for all three signals (L1, L2, L5 – shown in green, blue and red respectively). At the very beginning of the enhancement in S4 (at 19:18 UT), a spike in the IFLC, see panel b), is recorded. This is seen in the IFLC of L1, L5 (red) and the IFLC of L1, L2 (blue). At the same time as the IFLC spike, the auroral intensity peaks at 100 kR, see panel c). The  $\sigma_\phi$  index, shown in panel d), is elevated between 19:16 and 19:45 UT and therefore follows the behavior of the auroral intensity, see again panel c).

The simultaneous measurements of elevated S4,  $\sigma_\phi$  and IFLC indicate large and small-scale irregularities within the radio wave path. Not all auroral particle precipitation is leading to elevated S4. An elevated  $\sigma_\phi$  index during particle precipitation has been linked to E-region plasma instabilities. Elevated  $\sigma_\phi$  is predominately observed on the boundaries of the auroral forms, suggesting the Kelvin - Helmholtz or Farley - Buneman instability to play a role in the structuring processes causing it [7]. It remains open, how small-scale regularities affecting S4 indices form and which instabilities affect it. We will evaluate further under which conditions, such as auroral forms, emission altitude and electron energy, small-scale irregularities form, to try to understand how they form and their spatial and temporal evolution. For this we will expand our case study and use

multiple instruments to determine ionospheric plasma conditions.

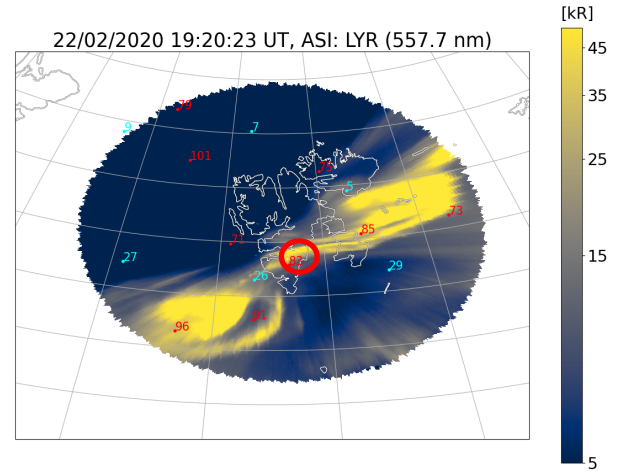


**Figure 1.** The projection of the 557.7 nm emissions shown together with the position of GPS (shown in blue) and GALILEO (shown in red) satellites over a map of Svalbard on 22<sup>nd</sup> February 2020 as seen from the LYR ASI. Brighter yellow auroral emissions mean stronger intensity.

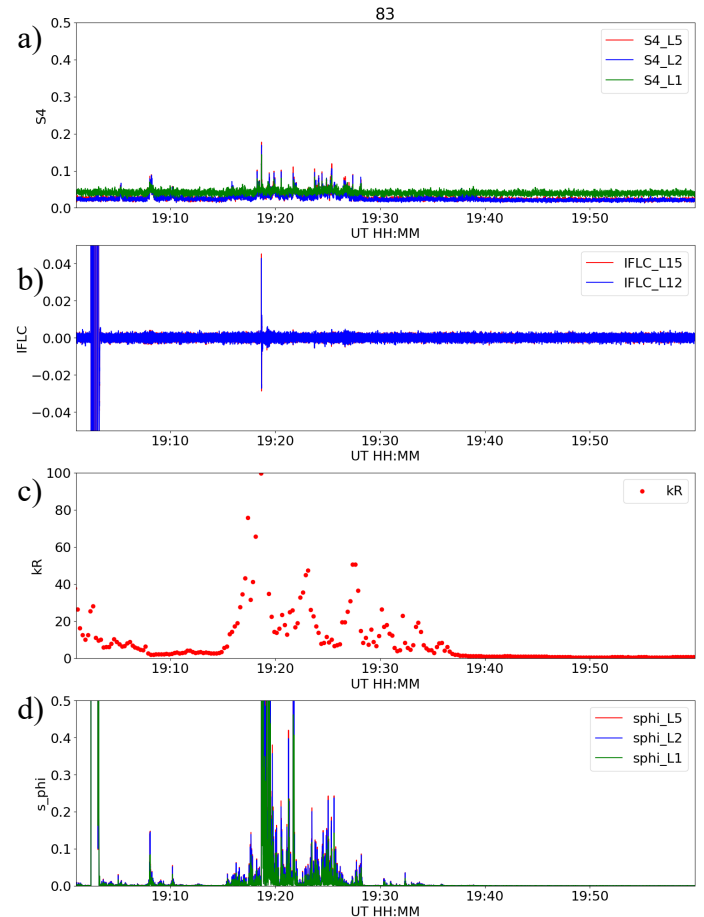


**Figure 2.** Data from the 22<sup>nd</sup> February 2020 from 18-20 UT. The scintillation indices S4 and  $\sigma_\phi$  are shown in panel a) and d), for the different frequencies (L1, L2, L5 – shown in green, blue and red). The IFLC is shown in panel b). It is calculated for L1 & L5 (see red line) and for L1 & L2 (see blue line). Panel c) shows the 557.7 nm emissions

intensity observed by the LYR ASI along the position of the satellite. A simultaneous peak of all indices in all panels is observed at about 19:18 UT. The indices quantify the location, scale, duration and intensity of plasma structuring.

## References

- [1] Kintner, P. M., Ledvina, B. M., and de Paula, E. R., "GPS and ionospheric scintillations", *Space Weather*, **5**, 9, September 2007, doi: 10.1029/2006SW000260.
- [2] Kung Chie Yeh and Chao-Han Liu, "Radio wave scintillations in the ionosphere", in *Proceedings of the IEEE*, **70**, 4, pp. 324-360, April 1982, doi: 10.1109/PROC.1982.12313.
- [3] Beach, T. L., "Perils of the GPS phase scintillation index ( $\sigma\phi$ )", *Radio Science*, **41**, 5, May 2006, doi:10.1029/2005RS003356.
- [4] Spogli, L., Ghobadi, H., Cicone, A., Alfonsi, L., Cesaroni, C., Linty, N., and Cafaro, M., "Adaptive phase detrending for gnss scintillation detection: A case study over Antarctica.", in *IEEE Geoscience and Remote Sensing Letters*, **19**, 1-5, April 2022, doi: 10.1109/LGRS.2021.3067727
- [5] Bougard B., Sleewaegen J. M., Spogli L., Veetil S. V., and Monico J. F., "CIGALA: Challenging the solar maximum in Brazil with PolaRxS," in *Proc. 24th Int. Tech. Meeting Satell. Division Inst. Navigat.*, 2011, **4**, pp. 2572–2579, available at: <http://hdl.handle.net/11449/73031>
- [6] Upper Atmosphere Physics and Radio Propagation Working Group, Cesaroni C., De Franceschi G., Marcocci C., Pica E., Romano V., Spogli L., "Electronic Space Weather upper atmosphere database (eSWua) - GNSS scintillation data, version 1.0.", Istituto Nazionale di Geofisicae Vulcanologia (INGV), 2020, <https://doi.org/10.13127/eswua/gnss>
- [7] Enengl F., Kotova D., Jin Y., Clausen L. B.N. and Miloch W.J., "Ionospheric plasma structuring in relation to auroral particle precipitation", *Journal Space Weather Space Climate*, **13**, 1, January 2022, doi: <https://doi.org/10.1051/swsc/2022038>